

# Molecular dynamic simulation of the $[N(C_4H_9)_4]BF_4 / (110) \alpha-Al_2O_3$ interface

Igor Gainutdinov \* , Nikolai Uvarov 

Institute of Solid State Chemistry and Mechanochemistry SB RAS, Novosibirsk 630090, Russia

\* Corresponding author: [ur1742@gmail.com](mailto:ur1742@gmail.com)



This paper belongs to the RKFМ'23 Special Issue: <https://chem.conf.nstu.ru/>.

Guest Editors: Prof. N. Uvarov and Prof. E. Aubakirov.

## Abstract

The structure and transport properties of the pure salt  $[N_4]BF_4$  and this salt located in the contact with the (110) surface of  $\alpha-Al_2O_3$  were studied using a MD computer simulation in order to reveal the effect of the salt/oxide interface on the structure and properties of the salt. The radial distribution functions of the ions and their mean square displacements were analyzed as a function of the temperature during the cooling of the salt. It was found that in all the cases anions are more mobile than cations. The molten phase of  $[N_4]BF_4$  tends to crystallize at temperature 420 K which is close to the experimental melting point. The salt located in the  $[N_4]BF_4/(110)Al_2O_3$  interface exhibits high values of anion self-diffusion coefficients which are higher by 1.2–2 orders of magnitude than in pure salt. This effect is likely to be caused by the formation of a layered atomic structure located within a characteristic thickness of 5 nm. Despite the structuring, the structure of the salt is amorphous, no crystallization-related effect is observed. The results of MD simulations agree with the experimental effect of the conductivity enhancement observed previously in  $[N_4]BF_4-Al_2O_3$  nanocomposites.

## Keywords

molecular dynamic simulation  
tetrabutylammonium  
borofluorate  
composite  
organic salts  
diffusion  
structure

Received: 03.07.23

Revised: 10.08.23

Accepted: 14.08.23

Available online: 16.08.23

## Key findings

- The structure and transport properties of the pure salt  $[N_4]BF_4$  and this salt located in the contact with (110) surface of  $\alpha-Al_2O_3$  were studied using a MD computer simulation.
- The molten phase of  $[N_4]BF_4$  tends to crystallize at temperature 420 K which is close to the experimental melting point. The salt near the interface does not tend to crystallize and remains to be amorphous.
- The anion self-diffusion coefficients in the salt located in the  $[N_4]BF_4/(110)Al_2O_3$  interface are higher by 1.2–2 orders of magnitude than that in the pure salt, which is in agreement with the experimental observations.

© 2023, the Authors. This article is published in open access under the terms and conditions of the Creative Commons Attribution (CC BY) license (<http://creativecommons.org/licenses/by/4.0/>).

## 1. Introduction

High-temperature plastic phases of organic salts combine properties of both crystals and ionic liquids. On the one hand, they have crystalline structure characterized by a long-range ordering, but on the other hand, these compounds exhibit a strong reorientation disorder and a high local mobility of molecular fragments [1, 2] typical for ionic liquids. The local motions may facilitate ionic transport. A relatively high ionic conductivity of  $10^{-6}$ – $10^{-3}$  S/cm has been reported for plastic phases of [3–14], but the mechanism of the ionic transport in such phases remains unknown.

Tetra-alkylammonium salts  $[R_4N]X$  (R = individual alkyl groups  $CH_3$ ,  $C_2H_5$ ,  $C_3H_7$ ,  $C_4H_9$ , etc., or their combinations,

X = halide anions;  $BF_4^-$ ,  $ClO_4^-$ , TFSI-anions, etc.) are typical ionic liquids in a molten state [15]. On cooling, tetrabutylammonium salts  $(C_4H_9)_4NX$  (X =  $Cl^-$ ,  $Br^-$ ,  $I^-$ ,  $BF_4^-$ ,  $ClO_4^-$ ) crystallize with the formation of reorientationally disordered high-temperature plastic phases, which transform into ordered low-temperature modifications under further cooling [12, 13, 14]. The melting entropy of these salts is lower or comparable that of the solid-state transition indicating a high disordering in the plastic phases [16, 17].

Tetrabutylammonium tetrafluoroborates  $[R_4N]BF_4$  are promising materials for low-temperature solid-state electrochemical devices due to the high electrochemical stability of both quaternary ammonium cations  $(R_4N)^+$  and  $BF_4^-$

anions. In particular, tetrabutylammonium tetrafluoroborate  $[(C_4H_9)_4N]BF_4$  (hereafter,  $[N_4]BF_4$ ) exhibit a conductivity of around  $10^{-6}$  S/cm in the high-temperature plastic phase at 150 °C [13]. According to  $^{19}F$  NMR data, the dominant charge carriers in this phase are  $BF_4^-$  anions [13]. The salt  $[N_4]BF_4$  has several polymorphic modifications, differing in the degree of conformational disorder in hydrocarbon chains and reorientation disordering of anions [17]. However, despite of a strong disordering in both cation and anion sub-lattices, the total ionic conductivity of the salt is rather low even in the plastic phase.

In order to increase the conductivity of the ionic salts, a heterogeneous doping technique can be used [18, 19], which leads to an increase of conductivity by several orders in magnitude. It is known that the introduction of nanocrystalline chemically inert additives to the salt matrix may result in a strong increase in the conductivity of the salts. There are two reasons for the conductivity enhancement in the obtained composite solid electrolytes: (i) the excess concentration of point defects, which form a double electrical layer near the ionic salt/oxide interface [18] and (ii) the formation of the amorphous layer of the ionic salt near the interface [19]. In micro-composites, excess point defects in the surface double layer seems to be a primary reason for the conductivity increase, whereas the ionic conductivity is caused by the contribution of the amorphous interface-induced phases in nanocomposites. To date, a number of experimental data have been reported for a conductivity enhancement in inorganic nanocomposites. In contrast, the conductivity of nanocomposites based on organic salts remains practically unstudied. Recently, it has been experimentally found that the introduction of nanocrystalline alumina into the  $[N_4]BF_4$  salt leads to a strong increase in the conductivity by several orders of magnitude. In parallel, the amorphization of the salt takes place at a high concentration of the alumina additive [20].

It would be very desirable to understand the mechanism of the effect of the heterogeneous doping on the structural and transport properties of the  $[N_4]BF_4$  salt. Previous studies [17] have shown that due to the branched structure of the tetrabutylammonium cations rotational motions of the fragments of hydrocarbon chains and changes in their conformation occur even at relatively low temperatures (about 200 K). Therefore, it is difficult to investigate the structure of the  $[N_4]BF_4$  salt by diffraction methods. The experimental study of the local structure of the salt near the ionic salt/oxide interface is even more complicated. In this situation, molecular dynamics (MD) computer simulation can provide an opportunity to obtain qualitative, and, possibly, quantitative information on the local structure of the salt in both individual form and in the composite. Previous MD simulations of salt-oxide interfaces have been carried out mainly for ionic liquids contacted with different oxide surfaces [21, 22]. As for composites with solid ionic salts, only  $LiI-Al_2O_3$  [23],  $CsCl-Al_2O_3$  [24] and  $Pb_{1-x}Cd_xF_2-SiO_2$  [25] interfaces were simulated. No data on MD simulations of

composite solid electrolytes with quaternary ammonium salts have been reported yet. Some efforts have been made to analytically solve the problem of crystallization of two-component systems, but they do not answer the question of increasing the ionic conductivity of organic salts in the composite [39–41].

This work is devoted to the MD computer modelling of the transport properties of pure  $[N_4]BF_4$  and this salt in contact with the (110) surface of  $\alpha-Al_2O_3$ .

## 2. Methodology

The calculations were performed with the LAMMPS software package [26] using the DREIDING force field [27]. The charges of the ions were refined by quantum chemical calculations of the molecule using the QUANTUM ESPRESSO package [28, 29]. The charges of the ions were determined by the Bader method [30]. It should be noted that the DREIDING force field is a rather early approach and there are now more advanced force fields available, but it has the advantage of allowing a consistent set of parameters to be defined for the system containing C, F, B, N, and H atoms within the same force field that has been developed and validated on a wide range of compounds.

A structure of a pure ionic salt containing 215 anion-cation pairs was simulated with periodic boundary conditions. In the present study only Coulomb interactions between atoms of different molecules and the Lennard-Jones dispersion attraction  $\sim \frac{1}{r^6}$  were considered. The intermolecular repulsion of atoms was also expressed in the Lennard-Jones form  $\sim \frac{1}{r^{12}}$ . No specific hydrogen bonds and cation polarization effects were taken in consideration. The boron atom in the  $BF_4^-$  anion ion is positively charged, its charge is equal to +2.4e and surrounded by four negatively charged fluorine ions (-0.84e). In the tetrabutylammonium cation, the nitrogen atom is negatively charged (-0.81e), while the charge of the carbon atoms fluctuates along the alkyl chains, the carbon atoms closest to the nitrogen have a charge of +0.17e, the hydrogen atoms have a small positive charge in the range of 0.02–0.1e.

Quantum chemical calculations show that under the action of the anionic electric field, the electron density is redistributed over the cation. Such a polarization effect was also neglected in the present simulation. Nevertheless, as it will be seen further, despite a significant simplification of the computational model, the obtained results in terms of characteristic temperatures, are in good agreement with the experimental data.

For simulations of the  $[N_4]BF_4/Al_2O_3$  interface, the modification  $\alpha-Al_2O_3$  (corundum, the symmetry space group  $R-3c$ , the lattice parameters  $a = b = 4.7602 \text{ \AA}$   $c = 12.9933 \text{ \AA}$ ) was used. The oxygen and aluminum ions were located in positions corresponding to the ideal corundum structure [31]. Both oxygen and aluminum positions are fixed and these ions act as rigid charged centers interacting due to

Coulomb and Lennard-Jones repulsive and attractive forces. Aluminum and oxygen ion charges were as assumed to be +1.8e and -1.2e, respectively.

### 3. Results and Discussion

#### 3.1. Pure $[N_4]BF_4$ salt

First, it was necessary to model the organic ionic salt. Its melting point is a thermodynamic parameter which can be easily determined experimentally. If the model shows a melting temperature close to the real one, then the interaction parameters used in the model are valid. For example, if hydrogen bonds between fluorine and hydrogen atoms play a significant role in the intermolecular interaction, then excluding them from the calculation would affect the melting temperature, in this case leading to its decrease. The same reasoning applies to the polarization of the cation.

It would be desirable to observe the melting temperature during heating the system. However, it is known that when a perfect crystal without defects is heated, the temperature of transition to a disordered state (the temperature of thermal instability) can be up to 20% higher than the melting temperature observed in the experiment [32]. Therefore, another approach was used: to melt the model and investigate the properties of the system in the course of its cooling from the molten state.

Figure 1 shows the mean square displacement of  $[N_4]^+$  cations and  $BF_4^-$  anions during a slow cooling of pure  $[N_4]BF_4$  salt from the molten state 550 K to 150 K with a constant cooling rate. In parallel, volume, energy, and the cell shape were monitored. Typically, the cooling process took nearly 10 ns ( $10^7$  time steps). The mean square displacement of atoms was calculated as the square of the deviation of the atoms from their initial positions (at the starting temperature) averaged over all atoms of the selected type. The mean square deviations of the boron atoms as the centers of the geometric position of the anion and the mean square deviations of all atoms included in the cation were monitored.

No drastic change in the volume and energy behavior with the temperature was observed. Changes in the state of the model during cooling are observed in the mean square displacement of atoms.

The mean square displacement of the atom at a fixed temperature is defined by the self-diffusion coefficient value,  $D \sim x^2/dt$ , which may be estimated from the slope of the time dependence of the mean square displacement. As seen from Figure 1, at high temperatures the diffusion coefficients of both cations and anions are rather high, but anions are more mobile than cations. With a decrease in temperature the  $dx^2/dt$  slope diminishes, hence the mobility of atoms monotonically decreases. However, at 420 K one can observe a sharp change in the  $dx^2/dt$  slope corresponding to a significant decrease in the mobility of both anions and cations. Interestingly, this temperature is close

to the experimental value of the melting temperature of 432 K [17].

Thus, the simulated mean square displacement curve reflects the freezing of a system at a temperature close to the crystallization point, but at the same time, the system has not crystallized, no long-range order has appeared, as can be seen from the pair distribution function (PDF) presented in Figure 2. In the PDF plots obtained at different moments of the cooling process (i.e. at different temperatures from 500 K to 150 K) one can see a broad first peak and slightly split second peak, which is a fingerprint of the disordered glassy structure.

Apparently, the process of establishing a long-range order is very slow at the crystallization (melting) temperature and the cooling rate that we can obtain in a computer experiment is too high. As a result, the system transforms to the quenched metastable glassy state. It is not surprising for the case of organic salt, which belongs to the class of plastic phases with a low value of entropy and enthalpy of melting and prone to amorphization for this reason.

#### 3.2. The $[N_4]BF_4/Al_2O_3$ interface

The  $[N_4]BF_4/Al_2O_3$  interface was simulated as follows: A plate of  $\alpha-Al_2O_3$  bounded by (110) planes, contacted with a layer of the  $[N_4]BF_4$  salt, containing 250 molecules (anion-cation pairs) placed on the alumina surface.

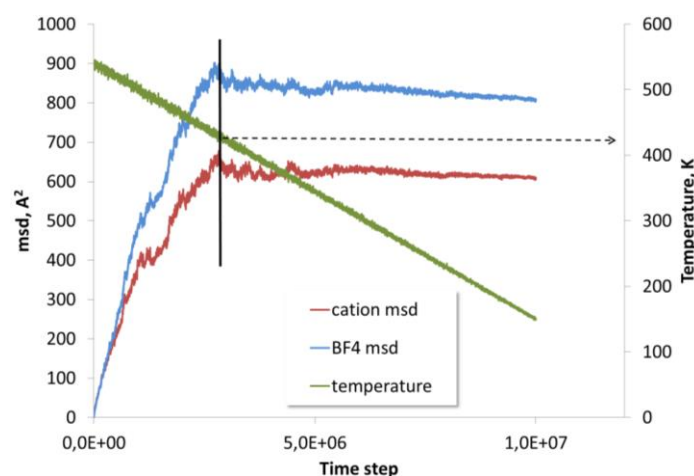


**Figure 1** Mean square displacement of boron atoms as centers of anions (blue) and for cation (brown) for pure  $[N_4]$  salt in comparison with temperature (green) during cooling run.

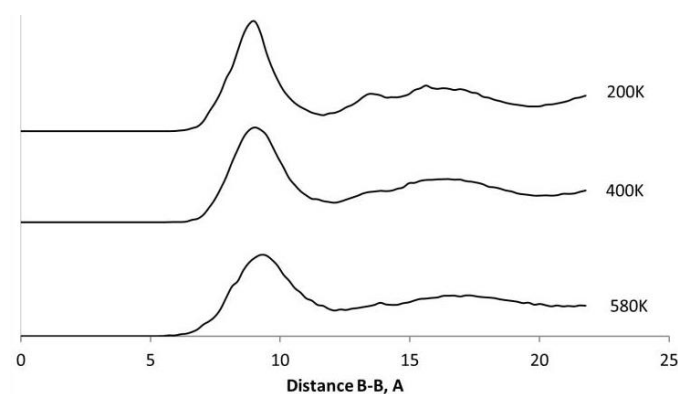


**Figure 2** Pair distribution function for boron for different temperatures during cooling process for pure  $[N_4]$ .

The bottom part of the salt layer contacted to the oxide surface, whereas the upper part formed a free surface (i.e., contacted to vacuum). If the  $z$  axis is perpendicular to the surface, then periodic boundary conditions were applied along the  $x$  and  $y$  axes.

As in the case of pure  $[\text{N}_4]\text{BF}_4$  salt, the model was heated up to 450 K and slowly cooled to 220 K with the same cooling rate. The time dependences of the mean square deviation of boron atoms and cations are shown in Figure 3.

In contrast to the pure  $[\text{N}_4]\text{BF}_4$  salt, the composite cooling from 450 to 220 K reveals no sharp changes in the mobility of atoms at 420 K (Figure 3). Mobility remains high and gradually decreases on cooling to 300 K. The distinction of the temperature dependence of atom mobilities in pure salt and the composite is apparently caused by a difference in the diffusion mechanism. This suggests the  $[\text{N}_4]\text{BF}_4$  salt in the contact with the alumina surface exists in an amorphous state which is different from the amorphous state of the pure salt.

Figure 4 shows the diffusion coefficients of boron atoms in the composite, as well as boron atoms in an infinite sample of pure salt  $[\text{N}_4]\text{BF}_4$ . The diffusion data for pure salt agree well with the bulk values of the self-diffusion coefficients,  $10^{-12}$ – $10^{-10}$   $\text{m}^2/\text{s}$ , obtained for various ionic liquids [33].

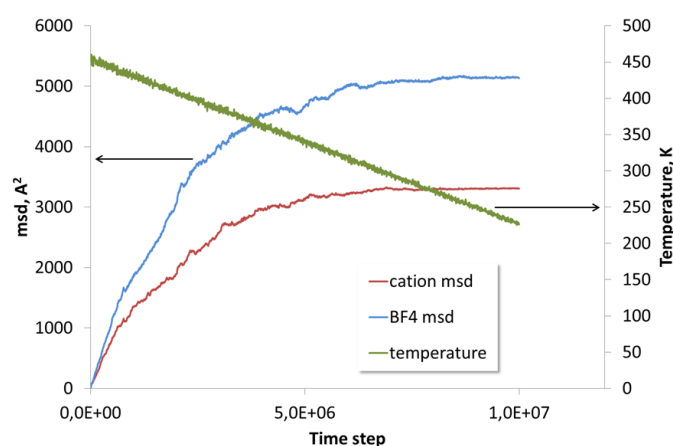


**Figure 3** Mean square displacement of boron atoms as centers of anions (brown) and for cation (blue) in comparison with temperature during cooling run for composite  $[\text{N}_4]\text{BF}_4\text{-Al}_2\text{O}_3$ .

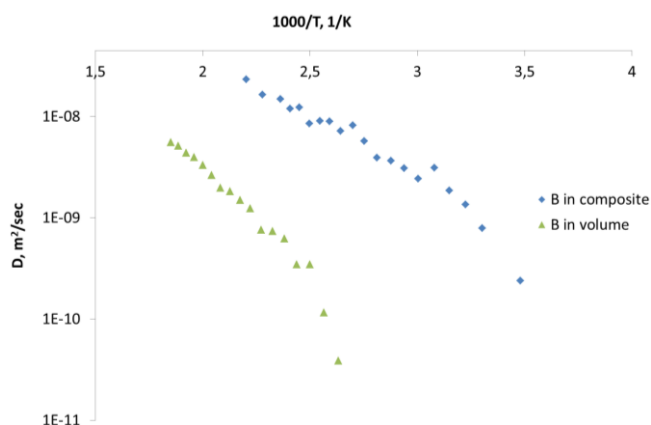


**Figure 4** Temperature dependences of boron self-diffusion coefficients in pure  $\text{N}_4\text{BF}_4$  salt (green triangles) and  $[\text{N}_4]\text{BF}_4\text{-Al}_2\text{O}_3$  composite (blue squares) estimated from MD simulations made on a cooling run.

In contrast, the diffusion coefficient of boron in the composite is by 1–2 orders of magnitude higher than the corresponding values for pure salt. At 420 K an abrupt decrease in the diffusion coefficient is observed for pure salt, while the  $D$  values for the composite monotonically decrease over the entire temperature range from 450 to 220 K.

The main factor affecting the structure and properties of the salt in the composite is the contact interaction between the oxide and salt. Due to Coulomb forces, this interaction is strong enough and leads to the formation of a surface layer in which the anions and cations of the salt are actually fixed on the surface of the oxide. They are practically stationary, and are arranged in such a way that the butyl chains of the cation lie on the surface in some flat conformation. The reason for such a strong difference in the atoms mobility in pure salt and in the composite seems to be the change in the local structure of the salt in the vicinity of the interface. Figure 5 shows the distribution of the boron atoms along the  $z$ -axis directed in perpendicular to the interface. In contrast to the pure  $[\text{N}_4]\text{BF}_4$  salt (Figure 2), several smooth single anionic layers can be distinguished in the salt structure near the  $[\text{N}_4]\text{BF}_4$  – alumina interface. Most likely that such a layered structure contains large two-dimensional cavities (“vacancies”) which act as an additional channel for fast ion transport along the interface. The characteristic thickness of the structured interface layer is nearly 5 nm that agrees with the effective thickness of the amorphous layer around the alumina particles estimated earlier for  $[\text{N}_4]\text{BF}_4\text{-Al}_2\text{O}_3$  nanocomposites using thermal analysis data [14].

The formation of layered structures is typical for the contacts between ionic liquids and oxides, metals, carbon nanotubes, etc. [21, 22, 38]. It has been reported [38] that an interfacial layer structure is formed near ionic liquids/ $\text{Al}_2\text{O}_3$  interfaces with different ionic liquids, indicating the formation of a double-layer consisting of cations being in contact with the anions repelled from the  $\text{Al}_2\text{O}_3$  surface and formed a second anion layer on the interfacial cation layer. Such a structure is completely different from those of dilute aqueous electrolytes near charged substrates, owing to strong correlations between oppositely charged ions. In most of the publications [21, 22, 38], the authors focused mainly on the structure and its influence on adhesion properties of the ionic liquids.

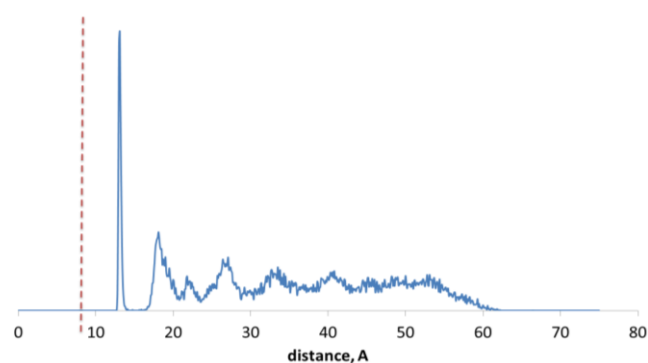


**Figure 5** The time averaged density of boron atoms along  $z$  axis at 290 K. The oxide surface is indicated by a dash line.

The effect of the structuring on ionic conductivity was not studied in detail. In this work such effect was clearly demonstrated for the case of ionic plastic phase/oxide interface.

#### 4. Limitations

The main difficulty of a fundamental nature is the adequacy of the choice of the model of interatomic interaction. On the one hand, for organic molecules, the method of force fields is well tested and is generally accepted. On the other hand, the approach chosen in this work ignores a number of features of these systems that may be important, in particular the polarization of the cation and anion as a whole, hydrogen bonds. In principle, to take into account the effect of changing charges depending on the environment, various empirical methods for the determination of effective charges during the calculation, QE, EAM, etc. [34–37] can be applied. Actually, it is planned to use these approaches in further studies.

The second difficulty concerns the size of the system. It is possible that in order to manifest a number of effects related to ion mobility, it is necessary to have a large computational domain. Only in this case the volume fluctuations necessary for the ion movements can occur. Such fluctuations are possible in the glassy state due to the excess free volume frozen into an amorphous structure, but when considering crystalline salts with a denser packing of molecules a low probability of fluctuations becomes critical when modeling diffusion displacements.

Finally, an important limitation is the physical observation time. Now it is limited by an interval of 10 ns, it is possible to increase this time by 2–3 times, but to move further one can carry out a computational experiment for several days. In any case, for a model of our size, a time of 100 ns seems to be a hard limit. Is it critical for the processes we are studying? This question requires careful study.

#### 5. Conclusions

In the present work, the structure and transport properties of the pure salt  $[N_4]BF_4$  and this salt located in the contact with  $\alpha-Al_2O_3$  were studied using a MD computer simulation in order to reveal the effect of the salt/oxide interface on the properties of the salt.

The radial distribution functions of the ions and their mean square displacements were analyzed as a function of the temperature during the cooling the salt. It was found that in the molten salt anions are more mobile than cations. The modelled molten phase of  $[N_4]BF_4$  tends to crystallize at temperature 420 K which is close to the experimental melting point of the salt (432 K). Due to a limited time interval of the calculations, we did not achieve a complete crystallization of the salt, but a strong decrease of the diffusion coefficients suggests that the phase transition takes place.

The  $[N_4]BF_4/(110)Al_2O_3$  interface was simulated and the properties of the salt were analyzed. It was found that in the contact with the oxide surface the salt exhibits high values of anions self-diffusion coefficients by higher 1.2–2 orders of magnitude than those in pure salt, anions being dominant charge carriers. This effect is likely caused by a structuring of the salt near the interface, i.e. the formation of a layered atomic structure located within a characteristic thickness of 5 nm. Despite the structuring, the salt remains to be amorphous with no tendency to crystallize over the temperature range from 550 to 300 K. The effect of the conductivity increase agrees with the experimental conductivity behavior of  $[N_4]BF_4-Al_2O_3$  nanocomposites observed earlier [20].

#### • Supplementary materials

No supplementary materials are available.

#### • Funding

The work was supported by the Russian Science Foundation (project 20-13-00302), <https://www.rscf.ru/en>.



#### • Acknowledgments

The Siberian Branch of the Russian Academy of Sciences (SB RAS) Siberian Supercomputer Center is gratefully acknowledged for providing supercomputer facilities.

#### • Author contributions

Conceptualization: I.G., N.U.

Data curation: I.G.,

Formal Analysis: I.G.,

Funding acquisition: N.U.

Investigation: I.G.

Methodology: I.G., N.U.

Project administration: N.U.

Resources: N.U.

Software: I.G.

Supervision: N.U.

Validation: I.G., N.U.

Visualization: I.G.

Writing – original draft: I.G., N.U.

Writing – review & editing: I.G., N.U.

#### • Conflict of interest

The authors declare no conflict of interest.

#### • Additional information

Author IDs:

Igor Gainutdinov, Scopus ID [37047923700](https://orcid.org/0000-0002-3704-7923);

Nikolai Uvarov, Scopus ID [7006949152](https://orcid.org/0009-0001-7006-9491).

Website:

Institute of Solid State Chemistry and Mechanochemistry, <http://www.solid.nsc.ru/>.

## References

1. Timmermans J. Plastic Crystals: A historical review. *J Phys Chem Solids*. 1961;18:1–8. doi:[10.1016/0022-3697\(61\)90076-2](https://doi.org/10.1016/0022-3697(61)90076-2)
2. Parsonage NG, Staveley LAK. Disorder in Crystals. International series of monographs on chemistry. Clarendon University Press: Oxford 1978. 926 p.
3. MacFarlane DR, Forsyth M. Plastic crystal electrolyte materials: new perspectives on solid state ionics. *Adv Mater*. 2001;13:957–966. doi:[10.1002/1521-4095\(200107\)13:12:13%3C957::AID-ADMA957%3E3.O.CO;2-%23](https://doi.org/10.1002/1521-4095(200107)13:12:13%3C957::AID-ADMA957%3E3.O.CO;2-%23)
4. Pringle JM, Howlett PC, MacFarlane DR, Forsyth M. Organic ionic plastic crystals: recent advances. *J Mater Chem*. 2010;20:2056–2062. doi:[10.1039/b920406g](https://doi.org/10.1039/b920406g)
5. Pringle JM. Recent progress in the development and use of organic ionic plastic crystal electrolytes. *Phys Chem Chem Phys*. 2013;15:1339–1351. doi:[10.1039/c2cp43267f](https://doi.org/10.1039/c2cp43267f)
6. Iwai S, Hattori M, Nakamura D, Ikeda R. Ionic dynamics in the rotator phase of n-alkylammonium chlorides (C<sub>6</sub>–C<sub>10</sub>), studied by <sup>1</sup>H nuclear magnetic resonance, electrical conductivity and thermal measurements. *J Chem Soc Faraday Trans*. 1993;89:827–831. doi:[10.1039/FT9938900827](https://doi.org/10.1039/FT9938900827)
7. Pas SJ, Huang J, Forsyth M, MacFarlane DR, Hill AJ. Defect-assisted conductivity in organic ionic plastic crystals. *J Chem Phys*. 2005;122:064704. doi:[10.1063/1.1845397](https://doi.org/10.1063/1.1845397)
8. Tanabe T, Nakamura D, Ikeda R. Novel ionic plastic phase of [(CH<sub>3</sub>)<sub>4</sub>N] SCN obtainable above 455 K studied by proton magnetic resonance, electrical conductivity and thermal measurements. *J Chem Soc Faraday Trans*. 1991;87:987–990. doi:[10.1039/ft9918700987](https://doi.org/10.1039/ft9918700987)
9. Seeber AJ, Forsyth M, Forsyth CM, Forsyth SA, Annat G, MacFarlane DR. Conductivity, NMR and crystallographic study of N, N, N, N-tetramethylammonium dicyanamide plastic crystal phases: an archetypal ambient temperature plastic electrolyte material. *Phys Chem Chem Phys*. 2003;5:2692–2698. doi:[10.1039/b212743a](https://doi.org/10.1039/b212743a)
10. Adebahr J, Grimsley M, Rocher NM, MacFarlane DR, Forsyth M. Rotational and translational mobility of a highly plastic salt: Dimethyl pyrrolidinium thiocyanate. *Solid State Ionics*. 2008;178:1793–1803. doi:[10.1016/j.ssi.2007.12.017](https://doi.org/10.1016/j.ssi.2007.12.017)
11. Asayama R, Kawamura J, Hattori T. Phase Transition and Ionic Transport Mechanism of (C<sub>4</sub>H<sub>9</sub>)<sub>4</sub>NI. *Chem Phys Letts*. 2005;414:87–91. doi:[10.1016/j.cplett.2005.08.055](https://doi.org/10.1016/j.cplett.2005.08.055)
12. Hayasaki T, Hirakawa S, Honda H. Investigation of new ionic plastic crystals in tetraalkylammonium tetrabutylborate. *Z Naturforsch*. 2014;69a:433–440. doi:[10.5560/zna.2014-0029](https://doi.org/10.5560/zna.2014-0029)
13. Uvarov NF, Iskakova AA, Bulina NV, Gerasimov KB, Slobovyuk AB, Kavun VYa. Ion conductivity of the plastic phase of the organic salt [(C<sub>4</sub>H<sub>9</sub>)<sub>4</sub>N]BF<sub>4</sub>. *Russ J Electrochem*. 2015;51:491–494. doi:[10.1134/S102319351505016X](https://doi.org/10.1134/S102319351505016X)
14. Isakova AA, Uliikhin AS, Uvarov NF, Gerasimov KB, Mateyshina YG. Comparative study of the ion conductivities of substituted tetrabutylammonium salts (C<sub>4</sub>H<sub>9</sub>)<sub>4</sub>N]BF<sub>4</sub> and [(C<sub>4</sub>H<sub>9</sub>)<sub>4</sub>N]. *Russ J Electrochem*. 2017;53:880–883. doi:[10.1134/S1023193517080079](https://doi.org/10.1134/S1023193517080079)
15. Zhang S, Lu X, Zhou Q, Li X, Zhang X, Li S. *Ionic liquids. Physicochemical Properties*, 1st ed.; Elsevier: Amsterdam, The Netherlands, 2009.
16. Uvarov NF, Asanbaeva NB, Ulihin AS, Mateyshina YG, Gerasimov KB. Thermal properties and ionic conductivity of tetra-n-butylammonium perchlorate. *Crystals*. 2022;12:515. doi:[10.3390/cryst12040515](https://doi.org/10.3390/cryst12040515)
17. Matsumoto K, Harinaga U, Tanaka R, Koyama A, Hagiwara R, Tsunashima K. The structural classification of the highly disordered crystal phases of [Nn][BF<sub>4</sub>], [Nn][PF<sub>6</sub>], [Pn][BF<sub>4</sub>], and [Pn][PF<sub>6</sub>] salts (Nn+ = tetraalkylammonium and Pn+ = tetraalkylphosphonium). *Phys Chem Chem Phys*. 2014;16:23616. doi:[10.1039/c4cp03391d](https://doi.org/10.1039/c4cp03391d)
18. Maier J. Ionic conduction in space charge regions. *Progr Solid State Chem*. 1995;23:171–263. doi:[10.1016/0079-6786\(95\)00004-E](https://doi.org/10.1016/0079-6786(95)00004-E)
19. Uvarov NF. Composite solid electrolytes: recent advances and design strategies. *J Solid State Electrochem*. 2011;15:367–389. doi:[10.1007/s10008-008-0739-4](https://doi.org/10.1007/s10008-008-0739-4)
20. Ulihin AS, Uvarov NF, Rabadanov KSh, Gafurov MM, Gerasimov KB. Thermal, structural and transport properties of composite solid electrolytes (1-x)(C<sub>4</sub>H<sub>9</sub>)<sub>4</sub>NBF<sub>4</sub>-xAl<sub>2</sub>O<sub>3</sub>. *Solid State Ionics*. 2022;378:115889. doi:[10.1016/j.ssi.2022.115889](https://doi.org/10.1016/j.ssi.2022.115889)
21. Wang YL, Li B, Sarman S, Mocci F, Lu ZY, Yuan J, Laaksonen A, Fayer MD. Microstructural and dynamical heterogeneities in ionic liquids. *Chem Rev*. 2020;120:5798–5877. doi:[10.1021/acs.chemrev.9b00693](https://doi.org/10.1021/acs.chemrev.9b00693)
22. Latorre CA, Ewen JP, Gattinoni C, Dini D. Simulating surfactant-iron oxide interfaces: from density functional theory to molecular dynamics. *J Phys Chem B*. 2019;123:6870–6881. doi:[10.1021/acs.jpcc.9b02925](https://doi.org/10.1021/acs.jpcc.9b02925)
23. Chung RHF, De Leeuw SW. Ionic conduction in LiI-α, γ-alumina: molecular dynamics study. *Solid State Ionics*. 2004;175:851–855. doi:[10.1016/j.ssi.2004.09.047](https://doi.org/10.1016/j.ssi.2004.09.047)
24. Gainutdinov II, Uvarov NF. Molecular dynamic simulation of the CsCl-Al<sub>2</sub>O<sub>3</sub> interface. *Solid State Ionics*. 2006;177:1631–1634. doi:[10.1016/j.ssi.2006.05.026](https://doi.org/10.1016/j.ssi.2006.05.026)
25. Petrov AV, Salamatov MS, Ivanov-Schitz AK. Effect of shape Si<sub>3</sub>O<sub>6</sub> clusters on fluoride diffusion in nanocomposites: computational evidence. *Ionics*. 2021;27:1255–1260. doi:[10.1007/s11581-020-03710-6](https://doi.org/10.1007/s11581-020-03710-6)
26. Plimpton SJ. Fast parallel algorithms for short-range molecular dynamics. *J Comp Phys*. 1995;117:1–19. doi:[10.1006/JCPH.1995.1039](https://doi.org/10.1006/JCPH.1995.1039)
27. Mayo SM, Olafson BD, Goddard III WA. DREIDING: A generic force field for molecular simulations. *J Phys Chem*. 1990;94:8897–8909. doi:[10.1021/j100389a010](https://doi.org/10.1021/j100389a010)
28. Giannozzi P, Baroni S, Bonini N, Calandra M, Car R, Cavazzoni C, Ceresoli D, Chiarotti GL, Cococcioni M, Dabo I, Dal Corso A, Fabris S, Fratesi G, de Gironcoli S, Gebauer R, Gerstmann U, Gougoussis C, Kokalj A, Lazzeri M, Martin-Samos L, Marzari N, Mauri F, Mazzarello R, Paolini S, Pasquarello A, Paulatto L, Sbraccia C, Scandolo S, Sclauzero G, Seitsonen AP, Smogunov A, Umari P, Wentzcovitch RM. QUANTUM ESPRESSO: a modular and open-source software project for quantum simulations of materials. *J Phys Condens Matter*. 2009;21:395502. doi:[10.1088/0953-8984/21/39/395502](https://doi.org/10.1088/0953-8984/21/39/395502)
29. Giannozzi P, Andreussi O, Brumme T, Bunau O, Nardelli MB, Calandra M, Car R, Cavazzoni C, Ceresoli D, Cococcioni M, Colonna N, Carnimeo I, Dal Corso A, de Gironcoli S, Delugas P, DiStasio Jr RA, Ferretti A, Floris A, Fratesi G, Fugallo G, Gebauer R, Gerstmann U, Giustino F, Gorni T, Jia J, Kawamura M, Ko H-Y, Kokalj A, Kucukbenli E, Lazzeri M, Marsili M, Marzari N, Mauri F, Nguyen NL, Nguyen H-V, Otero-de-la-Roza A, Paulatto L, Ponce S, Rocca D, Sabatini R, Santra B, Schlipf M, Seitsonen AP, Smogunov A, Timrov I, Thonhauser T, Umari P, Vast N, Wu X, Baroni S. Advanced capabilities for materials modelling with Quantum ESPRESSO. *J Phys Condens Matter*. 2017;29:465901. doi:[10.1088/1361-648X/aa8f79](https://doi.org/10.1088/1361-648X/aa8f79)
30. Yu M, Trinkle DR. Accurate and efficient algorithm for Bader charge integration. *J Chem Phys*. 2011;134:064111. doi:[10.1063/1.3553716](https://doi.org/10.1063/1.3553716)
31. Lewis J, Schwarzenbach D, Flack HD. Electric Field Gradients and Charge Density in Corundum, α-Al<sub>2</sub>O<sub>3</sub>. *Acta Crystallograph*. 1982;A38:733–739. doi:[10.1107/S0567739482001478](https://doi.org/10.1107/S0567739482001478)
32. Kapusta B, Guillope M. Molecular dynamics study of the perovskite MgSiO<sub>3</sub> at high temperature: structural, elastic and

- thermodynamical properties. *Phys Earth Planet.* 1993;75:205. doi:[10.1016/0031-9201\(93\)90002-Q](https://doi.org/10.1016/0031-9201(93)90002-Q)
33. Xiao Y, Song F, An S, Zeng F, Xu Y, Peng C, Liu H. Quantitative structure-property relationship for predicting the diffusion coefficient of ionic liquids. *J Molecular Liquids.* 2022;349:118476. doi:[10.1016/j.molliq.2022.118476](https://doi.org/10.1016/j.molliq.2022.118476)
34. Rappé A, Goddard W. Charge equilibration for molecular dynamics simulations. *J Phys Chem.* 1991;95:3358–3363. doi:[10.1021/j100161a070](https://doi.org/10.1021/j100161a070)
35. Nakano F. Parallel multilevel preconditioned conjugate-gradient approach to variable-charge molecular dynamics. *Computer Phys Commun.* 1997;104:59–69. doi:[10.1016/S0010-4655\(97\)00041-6](https://doi.org/10.1016/S0010-4655(97)00041-6)
36. Rick SW, Stuart SJ, BerneBJ. Dynamical fluctuating charge force fields: Application to liquid water. *J Chem Phys.* 1994;101:6141–6156. doi:[10.1063/1.468398](https://doi.org/10.1063/1.468398)
37. Verstraelen T, Van Speybroeck V, Waroquier M. The electro-negativity equalization method and the split charge equilibration applied to organic systems: Parametrization, validation, and comparison. *J Chem Phys.* 2009;131:044127. doi:[10.1063/1.3187034](https://doi.org/10.1063/1.3187034)
38. Mezger M, Schroder H, Reichert H, Schramm S, Okasinski JS, Schoder S, Honkimaki V, Deutsch M, Ocko BM, Ralston J, Rohwerder M, Stratmann M, Dosch H. Molecular layering of fluorinated ionic liquids at a charged sapphire (0001) surface. *Sci.* 2008;322:424–428. doi:[10.1021/acs.jpcc.9b02925](https://doi.org/10.1021/acs.jpcc.9b02925)
39. Chaurasiya V, Kumar D, Rai K, Singh J. Heat transfer analysis describing freezing of a eutectic system by a line heat sink with convection effect in cylindrical geometry. *Zeitschrift für Naturforschung A.* 2022;77(6):589–598. doi:[10.1515/zna-2021-0320](https://doi.org/10.1515/zna-2021-0320)
40. Chaurasiya V, Rai K N, Singh J. Heat transfer analysis for the solidification of a binary eutectic system under imposed movement of the material. *J Therm Anal Calorim.* 2022;147:3229. doi:[10.1007/s10973-021-10614-8](https://doi.org/10.1007/s10973-021-10614-8)
41. Chaurasiya V, Rai K N, Singh J. A study of solidification on binary eutectic system with moving phase change material. *Therm Sci Eng Progr.* 2021;25:101002. doi:[10.1016/j.tsep.2021.101002](https://doi.org/10.1016/j.tsep.2021.101002)